Fano resonances in prism-coupled multimode square micropillar resonators

Ho-Tong Lee, Linjie Zhou, and Andrew W. Poon

Department of Electrical and Electronic Engineering, Hong Kong University of Science and Technology, Clear Water Bay, Hong Kong Special Administrative Region, China

Received January 18, 2005

We report Fano resonances in a multimode square glass micropillar resonator; the resonances were obtained by using angle-resolved prism coupling. Our experiments reveal characteristically asymmetric line shapes of high-Q resonances and of detuned low-Q resonances in multimode reflection spectra. The asymmetric resonance line shapes evolve for an approximately π phase within a 0.5° range of reflection angles. We model our observed asymmetric multimode resonances by the far-field interference between a light wave that is evanescently coupled with a high-Q mode orbit and a coherent light wave that is refractively coupled with a detuned low-Q mode orbit. © 2005 Optical Society of America

OCIS codes: 230.5750, 260.5740.

Optical microresonators with sphere, ring, disk, or polygon shapes[1–5] have been attracting considerable interest for photonic information processing because of their compact size and high-Q resonances. Among these, two-dimensional micropillar (μ-pillar) resonators are particularly suited for nascent high-density integrated photonic circuits. Previously,[3] we reported obtaining nearly single-mode high-Q resonances in square glass μ-pillar resonators by use of an angle-resolved prism-coupling technique. We observed characteristically sharp asymmetric resonances that were due to the ubiquitous Fano resonance-like interference[6] between a single resonance mode and a coherent background. Such sharp asymmetric resonance line shapes can have high extinction ratios between the resonance peak and the characteristic Fano resonance dip and thus show good promise for wavelength-agile applications in biochemical sensing and optical switching.[7–9] Recently, Fano resonances were reported in various optical resonance configurations, including waveguide-coupled microcavities,[7,8] two-dimensional photonic crystal microcavity,[9] and spherical Bragg resonators.[10] Among these works,[3,7–10] analyses of Fano resonances focused on only single resonance modes.

Here we report our experiment on and theoretical modeling of Fano resonances in multimode (MM) resonance spectra of a square glass μ-pillar resonator. We employ angle-resolved prism coupling to resolve the MM Fano resonance line-shape evolution in the far field. We model the MM asymmetric resonances using multiple-beam interference between a light wave evanescently coupled with a high-Q mode orbit and a coherent light wave refractively coupled with a detuned low-Q mode.

The inset of Fig. 1 shows two ray orbits of different incident angles, θ_A and θ_B, coherently prism coupled with a MM square μ-pillar resonator. The two ray orbits can be wave-front matched[2] at detuned resonance wavelengths λ_A and λ_B. At λ_A (λ_B), a light wave coupled with ray orbit A (B) constitutes a resonance mode, whereas a light wave coherently coupled with ray orbit B (A) gives rise to a background. Fano resonances occur when the light waves from the resonant orbits and the coherent light waves from the off-resonant orbits interfere in the far field.

The experimental setup (Fig. 1) was detailed in Ref. 3. A 200-μm fused-silica square optical fiber with four rounded corners was used as our square μ-pillar resonator. We fixed the square fiber sidewall and the fused-silica prism flat surface in close proximity but not in contact. A Gaussian beam from a wavelength-tunable diode laser was focused with an $f/25$ cylinder lens, forming a line beam with an estimated cone angle near 2° and an estimated lateral width of ~50 μm in the cylinder prism origin. The incident angle θ was ~45°, near the silica–air critical angle $\theta_c \approx 43.9°$ (silica refractive index $n \approx 1.44$). Such θ favors input coupling to four-bounce ray orbits in a square μ-pillar resonator.[2] The prism-reflected light was collimated by another $f/25$ cylinder lens and col-

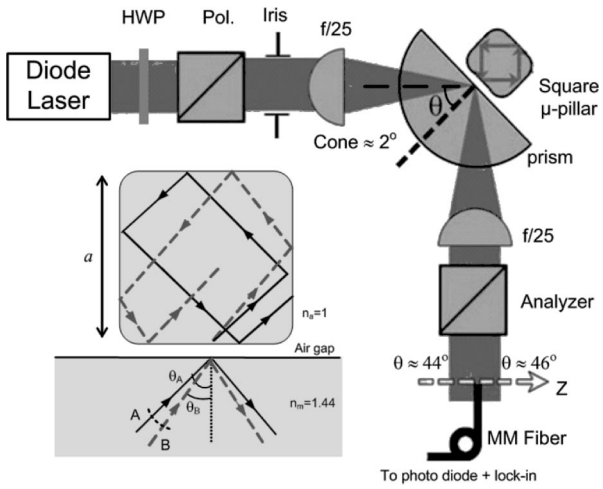

Fig. 1. Schematic of the experimental setup: The inset shows two coherently prism-coupled four-bounce ray orbits of a square μ-pillar resonator. n_a, air refractive index; n_m, dielectric medium refractive index; HWP, half-wave plate; Pol., polarizer; MM Fiber, multimode fiber; Z, MM fiber scanning direction.

0146-9592/05/121527-3/$15.00

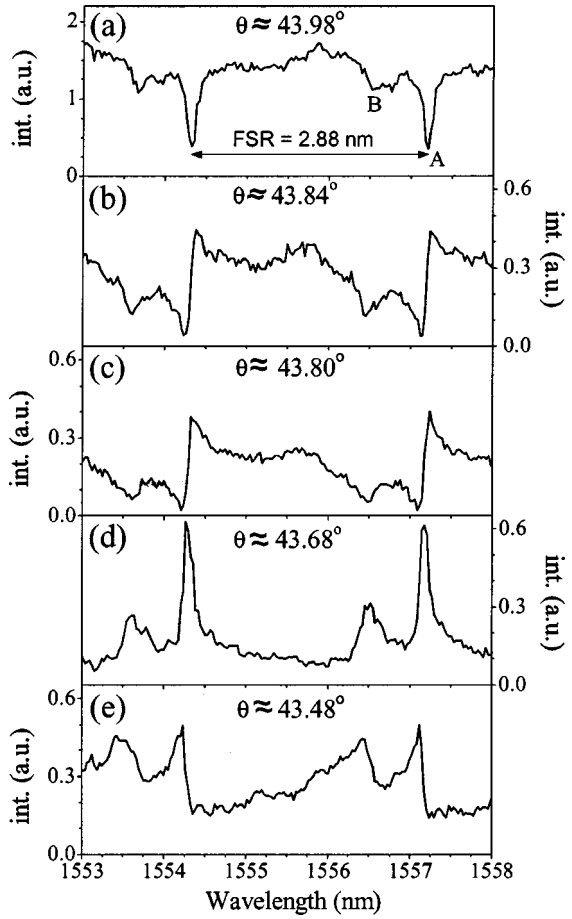

Fig. 2. Measured MM asymmetric resonance line shapes of $\theta \approx$ (a) 43.98°, (b) 43.84°, (c) 43.80°, (d) 43.68°, (e) 43.48°. int., intensity.

lected by a 62.5-μm-core MM fiber positioned by a translation stage after an analyzer. The scanning MM fiber (connected with a photodiode) made possible an angle-resolved measurement with an acceptance angle near 0.03°. The spectral resolution was ~0.02 nm, which was limited only by the wavelength-tuning steps. The angle-resolved measurement is essential to resolve the relative phase of light waves that are coherently coupled with MM resonance orbits and interfere in the far field.

Figure 2 shows the measured TM-polarized (**E** field along the square fiber axis) reflected spectra in the far field at various θ spanning 43.98°–43.48°. MM asymmetric resonances can be discerned. The line shapes evolve over an approximately π phase. Mode A has a Q of ~10,000, and mode B has a Q of ~6500. The free-spectral range of mode A is ~2.88 nm, and that of mode B is ~2.93 nm; both are consistent with the calculated free spectral range of $\approx$2.95 nm of a 45° four-bounce round-trip orbit with $n \approx 1.44$.[2]

Here we model the MM Fano resonances by the interference between a light wave that is evanescently coupled with a high-Q mode four-bounce orbit and a coherent light wave that is refractively coupled with a detuned low-Q mode four-bounce orbit. Figure 3 shows a schematic of our Fabry–Perot-like model. Given that the focused Gaussian beam comprises an angular distribution of plane waves (with an angular distribution near 2° about θ_c), it is possible that some of the plane-wave components are evanescently coupled [Fig. 3(a)], whereas some of the coherent plane-wave components are refractively coupled [Fig. 3(b)]. Figure 3(a) illustrates ray A evanescently coupled to a four-bounce wave-front-matched orbit with an incident angle θ_A that satisfies the square resonator total internal reflection (TIR) confinement condition $\theta_c < \theta_A < 90° - \theta_c$.[2] The reflected electric field complex amplitude E_A relative to the incident electric field amplitude E_0 can be expressed as follows[3]:

$$\frac{E_A}{E_0} = r_{\mathrm{FTIR}} + \frac{(t_{\mathrm{FTIR}})^2 \exp(i\phi_A)\exp(-\alpha L)}{1 - r_{\mathrm{FTIR}} \exp(i\phi_A)\exp(-\alpha L)}, \qquad (1)$$

where r_{FTIR} and t_{FTIR} are the frustrated TIR reflection and transmission complex coefficients at the air gap,[11] α is the cavity round-trip attenuation, and $L(\theta_A) = 2a(\sin\theta_A + \cos\theta_A)$ is the four-bounce wave-front-matched round-trip path length.[2] The phase angle ϕ_A is the phase change due to the wave-front-matched round-trip path length $L(\theta_A)$ and the Fresnel TIR phase shifts at the three sidewalls without coupling to the prism, and thus $\phi_A = nkL(\theta_A) + \gamma_R$, where $k = 2\pi/\lambda$ and $\gamma_R = \gamma(\theta_A) + 2\gamma(90° - \theta_A)$. At resonances, $\phi_A + \arg(r_{\mathrm{FTIR}}) = m2\pi$, where m is an integer and $\arg(r_{\mathrm{FTIR}})$ is the phase shift due to Fresnel TIR. The attenuation α represents cavity loss due to surface wave leakage, scattering loss, and coupling loss at the finite-length coupling interface.

Figure 3(b) illustrates ray B refractively coupled to a four-bounce wave-front-matched round-trip orbit with an incident angle $\theta_B < \theta_c$. Refractive leakage also occurs at the resonator sidewall opposite the input-coupled sidewall. The reflected electric field complex amplitude E_B relative to E_0 can be expressed as follows:

$$\frac{E_B}{E_0} = r_{FP} + \frac{(t_{FP})^2 r_{ma} \exp(i\phi_B)\exp(-\alpha' L)}{1 - r_{FP} r_{ma} \exp(i\phi_B)\exp(-\alpha' L)}, \qquad (2)$$

where r_{FP} and t_{FP} are the Fabry–Perot reflection and transmission complex coefficients at the air gap,[11] r_{ma}

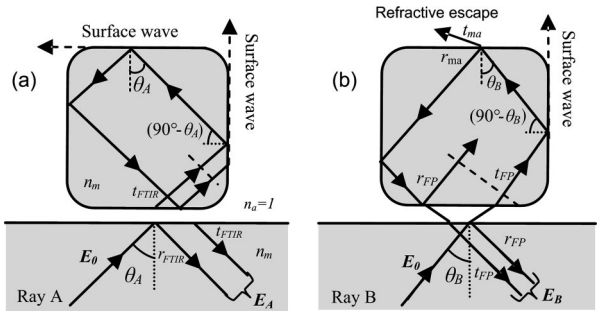

Fig. 3. (a) Schematic of an evanescently coupled four-bounce ray orbit in a square μ-pillar resonator. The dashed line represents wave-front matching upon a round trip. The dashed arrow represents the surface wave leakage along the resonator sidewall. (b) Schematic of a refractively coupled four-bounce ray orbit in a square μ-pillar resonator.

(t_{ma}) is the Fresnel reflection (transmission) coefficient at the dielectric medium–air interface, and α' is the cavity round-trip attenuation. The phase angle $\phi_B = nkL(\theta_B) + 2\gamma(90° - \theta_B)$ is the phase change due to the wave-front-matched round-trip path length $L(\theta_B)$ and the Fresnel TIR phase shifts at incident angle $(90° - \theta_B) > \theta_c$ at the two cavity sidewalls orthogonal to the input-coupled sidewall. At resonances, $\phi_B + \arg(r_{FP}) = m'2\pi$, where m' is an integer and $\arg(r_{FP})$ is the phase shift due to Fabry–Perot reflection.

The coherent fields E_A and E_B can overlap spatially in the far field and interfere. The far-field multiple-beam interference intensity I (normalized to the incident intensity I_0) is

$$\frac{I}{I_0} = \left|\frac{E_A}{E_0}\right|^2 + f^2\left|\frac{E_B}{E_0}\right|^2 + 2f\left|\frac{E_A}{E_0}\right|\left|\frac{E_B}{E_0}\right|\cos(\Phi_A - \Phi_B), \tag{3}$$

where f is the angle-dependent amplitude ratio and $(\Phi_A - \Phi_B)$ is the angle-dependent relative phase between spatially extended fields E_A and E_B at the far field. We assume that f is a constant within a subdegree angle range. At resonance wavelength λ_A that satisfies the resonance condition for orbit A, the interference represents a resonance mode field E_A that interferes with an off-resonance field E_B. The relative phase $(\Phi_A - \Phi_B)$ then determines the asymmetric resonance line shapes.

Figure 4 shows the calculated MM asymmetric resonance line-shape evolution using Eqs. (1)–(3) as $|\Phi_A - \Phi_B|$ varies from 0 to 1.1 π. We chose $a = 210$ μm, $n_m = 1.44$, $\theta_A = 44°$, $\theta_B = 42.7°$, $g = 2000$ nm, $\alpha = \alpha' = 2$ cm^{-1}, and $f = 1$. We find good qualitative agreement between the modeled MM asymmetric resonance line-shape evolution and the measured spectra (Fig. 2).

In conclusion, we have experimentally demonstrated Fano resonances in a multimode square micropillar resonator by use of an angle-resolved prism-coupling technique. We observed Fano-resonance-like interference between light waves coherently coupled to a high-Q mode as a resonance and to a low-Q mode as a background. The MM asymmetric resonance line shapes evolved over an approximately π phase within a 0.5° range of reflection angles. In contrast with our previous work on single Fano resonances based on the same physical system,[3] this Letter highlights the mechanism of MM Fano resonances that results from interference between coherent ray-orbits in multimode cavities. Such MM Fano resonances should be relevant to development of wavelength-agile devices employing MM optical cavities.

This study was substantially supported by grants from the Research Grants Council and the University Grants Council of the Hong Kong Special Administrative Region, China (projects HKUST6166/02E and HIA01/02.EG05). We thank Y. L. Pan and R. K. Chang of Yale University for providing the square glass fibers. A. W. Poon's e-mail address is eeawpoon@ust.hk.

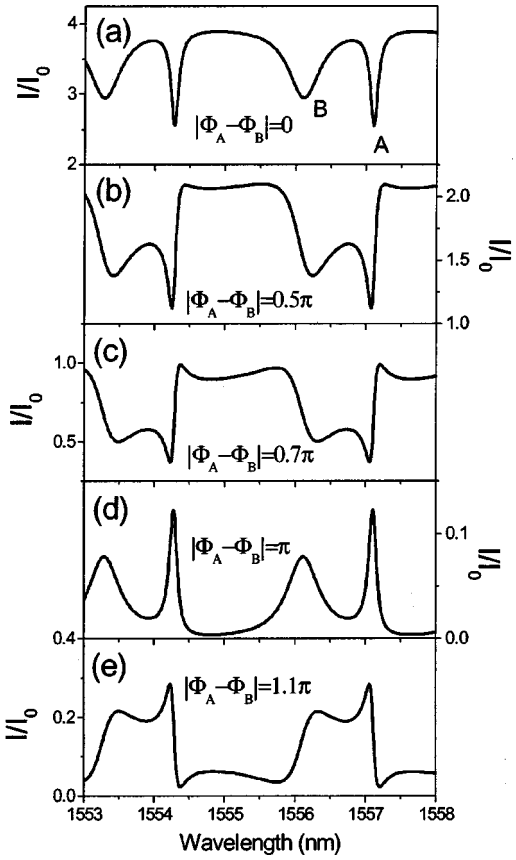

Fig. 4. Modeled MM asymmetric resonance line shapes: (a) $|\Phi_A - \Phi_B| = 0$, (b) $|\Phi_A - \Phi_B| = 0.5\pi$, (c) $|\Phi_A - \Phi_B| = 0.7\pi$, (d) $|\Phi_A - \Phi_B| = \pi$, (e) $|\Phi_A - \Phi_B| = 1.1\pi$.

References

1. K. J. Vahala, Nature **424**, 839 (2003).
2. A. W. Poon, F. Courvoisier, and R. K. Chang, Opt. Lett. **26**, 632 (2001).
3. H. T. Lee and A. W. Poon, Opt. Lett. **29**, 5 (2004).
4. N. Ma, C. Li, and A. W. Poon, IEEE Photonics Technol. Lett. **16**, 2487 (2004).
5. C. Li and A. W. Poon, Opt. Lett. **30**, 546 (2005).
6. U. Fano, Phys. Rev. **124**, 1866 (1961).
7. S. Fan, Appl. Phys. Lett. **80**, 908 (2002).
8. C. Y. Chao and L. J. Guo, Appl. Phys. Lett. **83**, 1527 (2003).
9. V. Lousse and J. P. Vigneron, Phys. Rev. B **69**, 155106 (2004).
10. W. Liang, Y. Xu, Y. Huang, A. Yariv, J. G. Fleming, and S. Y. Lin, Opt. Express **12**, 657 (2004).
11. M. Born and E. Wolf, *Principles of Optics*, 7th ed. (Cambridge U. Press, Cambridge, UK, 1999).